ARTICLE
Journal of Cellular Biochemistry 113:1671–1680 (2012)

Journal of Cellular Biochemistry

# Proteomic Investigation of 5-Fluorouracil Resistance in a Human Hepatocellular Carcinoma Cell Line

Shi-Wen Tong, Yi-Xuan Yang, Huai-Dong Hu, Xuan An, Feng Ye, Peng Hu, Hong Ren, Sang-Lin Li,* and Da-Zhi Zhang*

*Key Laboratory of Molecular Biology for Infectious Diseases of Ministry of Education of China, The Second Affiliated Hospital, Chongqing Medical University, Chongqing 400016, China*

## ABSTRACT

Multi-drug resistance (MDR) is a major obstacle towards a successful treatment of hepatocellular carcinoma (HCC). The mechanisms of MDR are intricate and have not been fully understood. Therefore, we employed a cell-line model consisting of the 5-fluorouracil (5-FU) resistant BEL7402/5-FU cell line and its parental BEL7402 cell line. Using relative and absolute quantification (iTRAQ)-coupled 2D LC-MS/MS, a successfully exploited high-throughput proteomic technology, in total, 660 unique proteins were identified and 52 proteins showed to be differentially expressed in BEL7402/5-FU compared with BEL7402. Several differentially expressed proteins were further validated by Western blot and real-time quantitative RT-PCR analysis. Furthermore, the association of MDR with ANXA3, one of the highly expressed proteins in BEL7402/5-FU, was verified. Our study represents the first successful application of iTRAQ technology for MDR mechanisms analysis in HCC. Many of the differentially expressed proteins identified had not been linked to MDR in HCC before, which provide valuable information for further understanding of MDR. J. Cell. Biochem. 113: 1671–1680, 2012. 

**KEY WORDS:** MULTI-DRUG RESISTANCE; HEPATOCELLULAR CARCINOMA; iTRAQ; MASS SPECTROMETRY

Worldwide, hepatocellular carcinoma (HCC) has risen to become the third leading cause of cancer-related mortality, which causes more than 600,000 deaths annually [Parkin et al., 2001]. A majority of patients with HCC are surgically unresectable because of their advanced stage of cancer at the time of diagnosis. Consequently, chemotherapy plays an important role in the treatment of HCC. Unfortunately, HCC generally responds poorly to chemotherapy owing to the development of the multiple drug resistance (MDR) [Schwartz et al., 2002]. MDR is a phenomenon in which cancer cells exposed to one anti-cancer drug become resistant to various other anti-cancer drugs that are structurally and functionally different from the initial chemotherapy [Perez-Tomas, 2006]. Several mechanisms have been found to be responsible for MDR such as increased drug efflux, DNA repair activity, and altered survival and apoptotic signaling pathways [Kusuhara et al., 1997; Morrow et al., 1998, 2000]. Although these pathogenesis studies on MDR of tumors have been undertaken successfully, the mechanisms of MDR are intricate and have not been fully elucidated yet [Yang et al., 2008].

5-Fluorouracil (5-FU) has been used to treat various cancers and accepted worldwide as a first-line anti-cancer drug for HCC chemotherapy. However, its usage is limited because of the rapid development of MDR. It is necessary to explore the mechanism underlying the resistance. 5-FU resistant cell line BEL7402/5-FU, which is derived from its parental HCC BEL7402 cell line by stepwise selection in vitro using 5-FU, and can also display cross-resistance to other anti-cancer drugs such as adriamycin and cytarabine, is a useful cell model for investigating the mechanisms underlying MDR in HCC [Jin et al., 2002]. Though the over-expression of P-gp was highly correlated with MDR phenotype in most cancer cells, however, the previous study revealed that BEL7402 and BEL7402/5-FU cells showed no difference in P-gp level, which indicated other resistance mechanisms might be involved in the development of MDR in BEL7402/5-FU. Further understanding of the molecular

Shi-Wen Tong, Yi-Xuan Yang and Huai-Dong Hu, contributed equally to this work.

Grant sponsor: Changjiang Scholars and Innovative Research Team in University; Grant number: IRT0872; Grant sponsor: National Natural Science Foundation of China; Grant numbers: 30930082, 30771923, 30801348, 30900507; Grant sponsor: National Science and Technology Major Project of China; Grant number: 2008ZX10002-006; Grant sponsor: China Postdoctoral Science Foundation Founded Project; Grant number: 20070410210.

*Correspondence to: Dr. Sang-Lin Li, or Prof. Da-Zhi Zhang, Key Laboratory of Molecular Biology for Infectious Diseases of Ministry of Education of China, the Second Affiliated Hospital, Chongqing Medical University, Chongqing, China. E-mail: sanglinli2001@163.com; dzhzhang@yahoo.com

Received 12 July 2011; Accepted 13 December 2011 • DOI 10.1002/jcb.24036 • © 2011 Wiley Periodicals, Inc.
Published online 20 December 2011 in Wiley Online Library (wileyonlinelibrary.com).

mechanism of MDR is likely to provide treatment that is more effective for the patients with HCC.

Over the past 5 years there has been an increasing interest in applying isotope-based quantitative proteomics for research of diverse nature—ranging from biomarker discovery to post-translational modifications. These emerging technologies include ICAT, relative and absolute quantification (iTRAQ), and $^{18}O$, and stable isotope labeling with amino acids in cell culture (SILAC) [Fu et al., 2009; Ho et al., 2009; Rangiah et al., 2009]. Among them iTRAQ method is a powerful tool in which up to eight samples can be analyzed in one experiment. Using this approach, we identified 52 differentially expressed proteins between 5-FU resistant cell line BEL7402/5-FU and BEL7402, and further functional studies suggested ANXA3 could be related to MDR, which may lead to a better characterization of the BEL7402/5-FU cell line, and therefore a better understanding of its multi-drug resistant phenotype.

## MATERIALS AND METHODS

### CELL LINES

5-FU resistant human HCC cell line BEL7402/5-FU and its parental cell line BEL7402 were purchased from the Cancer Research Department, China Medical Science Institute. BEL7402 was cultured with RPMI1640 medium containing 10% fetal calf serum (Gibco BRL, Grand Island, NY). To maintain biologic characteristics of MDR, BEL7402/5-FU was cultured with RPMI1640 medium containing 10% fetal calf serum and 100 mg/L 5-FU (Sigma–Aldrich, St. Louis, MO).

### TISSUE SAMPLES

Frozen tissues from HCC patients were obtained from the Second Affiliated Hospital of Chongqing Medical University. The tissue samples were from 14 males and 6 females, ages between 40 and 69 years old, and representing TNM stages I–IV. The sample set consisted of 20 HCC tissues and 20 matched normal liver tissues. Prior local ethics committee approval and informed patient consent were obtained in all cases.

### REAGENTS

The iTRAQ kits were purchased from Applied Biosystems (Foster City, CA). Sequence grade modified trypsin was purchased from Promega (Madison, WI). PVDF membrane, goat anti-mouse, goat anti-rabbit, or rabbit anti-goat IgG-conjugated with horseradish peroxidase, and the enhanced chemiluminescence (ECL) system were purchased from Amersham Biosciences (Uppsala, Sweden). Monoclonal or polyclonal antibodies against MARCKSL1, ANXA3, S100A14, ANXA2, CKB, and actin were from Santa Cruz Biotechnology (Santa Cruz, CA).

### TOXICITY TESTING

The cytotoxicity was determined using MTT assay and crystal violet assay described previously [Flick and Gifford, 1984; Plumb et al., 1989]. Briefly, the BEL7402/5-FU cells and BEL7402 cells were seeded in each well of 96-well plates for 24 h before use. The 5-FU, cisplatin, adriamycin, and vincristine of different concentrations were then added to the cells, and the cells were cultured for 72 h before the cell viability examination using both MTT assay and crystal violet assay. The concentration of drug causing 50% kill (IC50 of the drug) was determined by probit analysis on the SPSS 10.0 software (Chicago, IL).

### MEASUREMENT OF APOPTOSIS

Apoptosis induced by treatment with 5-FU (100 mg/L) was assayed at 24 h after treatment by using an AnnexinV-FITC/PI Apoptosis Detection Kit (BD Pharmingen) according to standard protocol. The experiment was repeated three times.

### PROTEIN SAMPLE PREPARATION AND iTRAQ LABELING

The cells were harvested, and lysed in lysis buffer (7 M urea, 1 mg/ml DNase I, 1 mM $Na_3VO_4$, and 1 mM PMSF). The lysates were incubated at 37°C for 1 h, and then centrifuged at 15,000 rpm for 30 min at 4°C. The supernatant was collected and the concentration of the total proteins was determined using 2D Quantification Kit (Amersham Biosciences). For each sample, a total of 100 μg of protein was precipitated by the addition of four volumes of cold acetone and stored at −20°C for 2 h. The precipitated protein was then dissolved in solution buffer, denatured, and cysteines blocked according to the manufacturer's instructions (Applied Biosystems). Each sample was then digested with 20 μL of 0.25 μg/μL trypsin (Promega) solution at 37°C overnight and labeled with the iTRAQ tags as follows: (i) parental cell line BEL7402-116 and -118 tags and (ii) 5-FU-resistant cell line BEL7402/5-FU-117 and -119 tags. The labeled samples were pooled prior to further analysis.

### STRONG CATION EXCHANGE CHROMATOGRAPHY

To reduce sample's complexity during LC-MS/MS analysis, the pooled samples were diluted 10-fold with SCX buffer A (10 mM $KH_2PO_4$ in 25% acetonitrile at pH 3.0) and subjected to a 2.1 × 200 $mm^2$ polysulfoethyl A SCX column (Poly LC, Columbia, MD). The column was eluted with a gradient of 0–25% SCX buffer B (10 mM $KH_2PO_4$ at pH 3.0 in 25% acetonitrile containing 350 mM KCl) over 30 min, followed by a gradient of 25–100% SCX buffer B over 40 min. The fractions were collected at 1 min intervals. These SCX fractions were lyophilized in a vacuum concentrator, and subjected to C-18 clean-up using a C18 Discovery® DSC-18 SPE column (100 mg capacity, Supelco, Sigma–Aldrich). The cleaned fractions were then lyophilized again and stored at −20°C prior to mass spectrometric analysis.

### ESI-Q-TOF-MS ANALYSIS AND DATA PROCESSING

Mass spectrometric analysis was performed using a nano-LC coupled online to QStarXL mass spectrometer (Applied Biosystems). Peptides were loaded on a 75 μm × 15 cm, 3 μm fused silica C18 capillary column, followed by mobile phase elution: buffer A (0.1% formic acid in 2% acetonitrile) and buffer B (0.1% formic acid in 98% acetonitrile). The peptides were eluted from 2% buffer B to 100% buffer B over 60 min at a flow rate 300 nL/min. The LC eluent was directed to ESI source for Q-TOF-MS analysis. The mass spectrometer was set to perform information-dependent acquisition (IDA) in the positive ion mode, with a selected mass range of 300–2,000 m/z. Peptides with +2 to +4 charge states were selected for tandem mass spectrometry, and the time of summation of MS/MS

events was set to 3 s. The two most abundantly charged peptides above a 10 count threshold were selected for MS/MS and dynamically excluded for 60 s with ±50 mmu mass tolerance.

Peptide identification and quantification were performed using ProteinPilot software packages (Applied Biosystems). Each MS/MS spectrum was searched against the IPI human protein database v3.49 and protein identification was accepted based on ProteinPilot confidence scores. Relative quantification of proteins, in the case of iTRAQ, is performed on the MS/MS scans and is the ratio of the areas under the peaks at 116, 117,118, and 119 Da, which were the masses of the tags that correspond to the iTRAQ reagents. Error factor (EF) and *P*-value are calculated using ProteinPilot software which gave an indication of the deviation and significance in the protein quantification.

### REAL-TIME QUANTITATIVE RT-PCR ANALYSIS

Total RNA was extracted using Trizol (Gibco BRL) following the manufacturer's instructions. Two micrograms of total RNA was reverse-transcribed into first-strand cDNA using A3500 Reverse Transcription System (Promega). Quantitative RT-PCR was performed on the ABI 7900HT system using the Taq-Man Gene Expression Assay Kit and gene-specific primers for 18S (Hs99999901_s1), MARCKSL1 (Hs00702769_s1), ANXA3 (Hs00971411_m1), S100A14 (Hs00221080_m1), GDI1 (Hs00181741_m1), ANXA2 (Hs00733393_m1), S100A10 (Hs00751478_s1), ANXA5 (Hs00154054_m1), HDGF (Hs00610314_m1), RAP1B (Hs00763004_s1), CKB (Hs01058288_g1), and FEN1 (Hs00254008_m1). The relative quantification of gene expression was analyzed by the $2^{-\Delta\Delta CT}$ method [Livak and Schmittgen, 2001]. Real-time quantitative RT-PCR analysis was repeated at least three times.

### WESTERN BLOT ANALYSIS

The cells were lysed at 4°C for 30 min in a lysis buffer (50 mM Tris, pH 7.4, 100 mM $NaCl_2$, 1 mM $MgCl_2$, 2.5 mM $Na_3VO_4$, 1 mM PMSF, 2.5 mM EDTA, 0.5% Triton X-100, 0.5% NP-40, 5 μg/ml of aprotinin, pepstatin A, and leupeptin). The cell lysates were centrifuged at 15, 000 rpm for 15 min at 4°C. Protein concentration was determined using 2D Quantification Kit (Amersham Biosciences). The protein samples (about 20 μg) were separated using SDS–PAGE. After SDS–PAGE electrophoresis, proteins were transferred to PVDF membranes. The membranes were blocked overnight at 4°C with 5% non-fat dry milk in TBS-T buffer (20 mM Tris, pH 7.6, 100 mM $NaCl_2$, 0.5% Tween-20), followed by 3 h of incubation with the primary antibody (1:1,500–1:2,000 dilution) in TBS-T buffer containing 5% non-fat dry milk at room temperature. After washing three times with TBS-T buffer, the membranes were incubated with a horseradish peroxidase-conjugated goat anti-mouse IgG, goat anti-rabbit IgG or rabbit anti-goat IgG as a secondary antibody (1:3,000 dilution) for 1 h at room temperature. The membranes were then washed three times in TBS-T buffer and the reactions were visualized with ECL detection system. All of the Western blot analyses were repeated at least three times.

### ADMINISTRATION OF ANXA3 siRNA TO CELLS

For functional studies, two siRNA duplexes against human ANXA3 (HSS100504 and HSS100506) and control siRNA were obtained from Invitrogen. The cells were transfected with siRNA according to the siRNA transfection protocol provided by the manufacturer. Briefly, BEL7402/5-FU cells were plated into 6-well plates and 96-well plates at the density of $10^5$ cells/ml medium, respectively. When the cells were 60–80% confluent, they were transfected with 20 nmol/L of ANXA3 siRNA, and control siRNA after a pre-incubation for 20 min with lipofectamine 2000 transfection reagent in Opti-MEM® I medium (Gibco). After 4 h of transfection, the medium was replaced with RPMI1640 medium containing 10% fetal calf serum, and continued to culture the cells for additional 44 h. The cells were then incubated with IC50 concentrations of 5-FU, cisplatin, adriamycin, or vincristine. After 72-h incubation, ANXA3 expression level was determined by Western blot analysis described above, and the cell viability of BEL7402/5-FU was examined using MTT assay and crystal violet assay.

### IMMUNOHISTOCHEMISTRY

Immunohistochemistry (IHC) of HCC was performed as described previously [Yang et al., 2010]. Briefly, frozen tissues were freshly prepared for IHC by fixing in 10% neutral buffered formalin for 16 h at 4°C, subjecting to a Thermo Shandon tissue processor, and embedding in paraffin. Sections were warmed in a 60°C oven, dewaxed in three changes of xylene, and passaged through graded ethanol (100%, 95%, and 70%) before a final wash in double distilled $H_2O$. After quenching of endogenous peroxidase activity with 3% $H_2O_2$ for 10 min and blocking with BSA for 30 min, sections were incubated at 4°C overnight with antibodies against ANXA3 at a 1:200 dilution. Detection was achieved with the Envision/horseradish peroxidase System (Dako-Cytomation). All slides were counterstained with Gill's Hematoxylin for 1 min, dehydrated, and mounted for light microscopic evaluation.

### STATISTICAL ANALYSIS

The data were expressed as mean ± SD, and analyzed with the Student's *t*-test between two groups. It was considered statistically significant if *P*-value was less than 0.05.

## RESULTS

### BIOLOGICAL CHARACTERISTICS OF BEL7402/5-FU CELLS

After cells were treated with different concentrations of 5-FU for 72 h, dose–response curves were plotted and analyzed using the probit model in SPSS 10.0 software (Table I). The IC50 values for 5-FU treatment in BEL7402/5-FU and BEL7402 cells were 673.77 ± 55.52 mg/L and 2.84 ± 0.36 mg/L, respectively, which meant the resistance of BEL7402/5-FU to 5-FU was 237.24-fold higher than that of BEL7402 cells (Fig. 1A and Table I). The anti-apoptotic activity was also measured via V-FITC/PI Apoptosis Detection Kit using flow cytometry (Fig. 1B). After treatment with 100 mg/L 5-FU, the apoptotic rate of BEL7402 was much higher than that of BEL7402/5-FU, suggesting that BEL7402/5-FU showed more resistance to 5-FU. In addition, both cell lines were also treated with different concentrations of other agents and results revealed resistance of BEL7402/5-FU to cisplatin, adriamycin, and vincristine significantly increased compared with BEL7402 cells, indicating the resistant cell, BEL7402/5-FU, induced by 5-FU, was a typical MDR

TABLE I. IC50 Values (mg/L) for Selected Regents (mean ± SD)

| Regent | BEL7402 | BEL7402/5-FU | Fold resistance relative to BEL7402 | *P*-value |
|---|---|---|---|---|
| 5-FU | 2.84 ± 0.36 | 673.77 ± 55.52 | 237.24 | <0.05 |
| Cisplatin | 8.02 ± 0.35 | 96.36 ± 6.85 | 12.01 | <0.05 |
| Adriamycin | 6.21 ± 0.76 | 167.05 ± 15.51 | 26.90 | <0.05 |
| Vincristine | 9.37 ± 1.07 | 84.21 ± 3.78 | 8.99 | <0.05 |

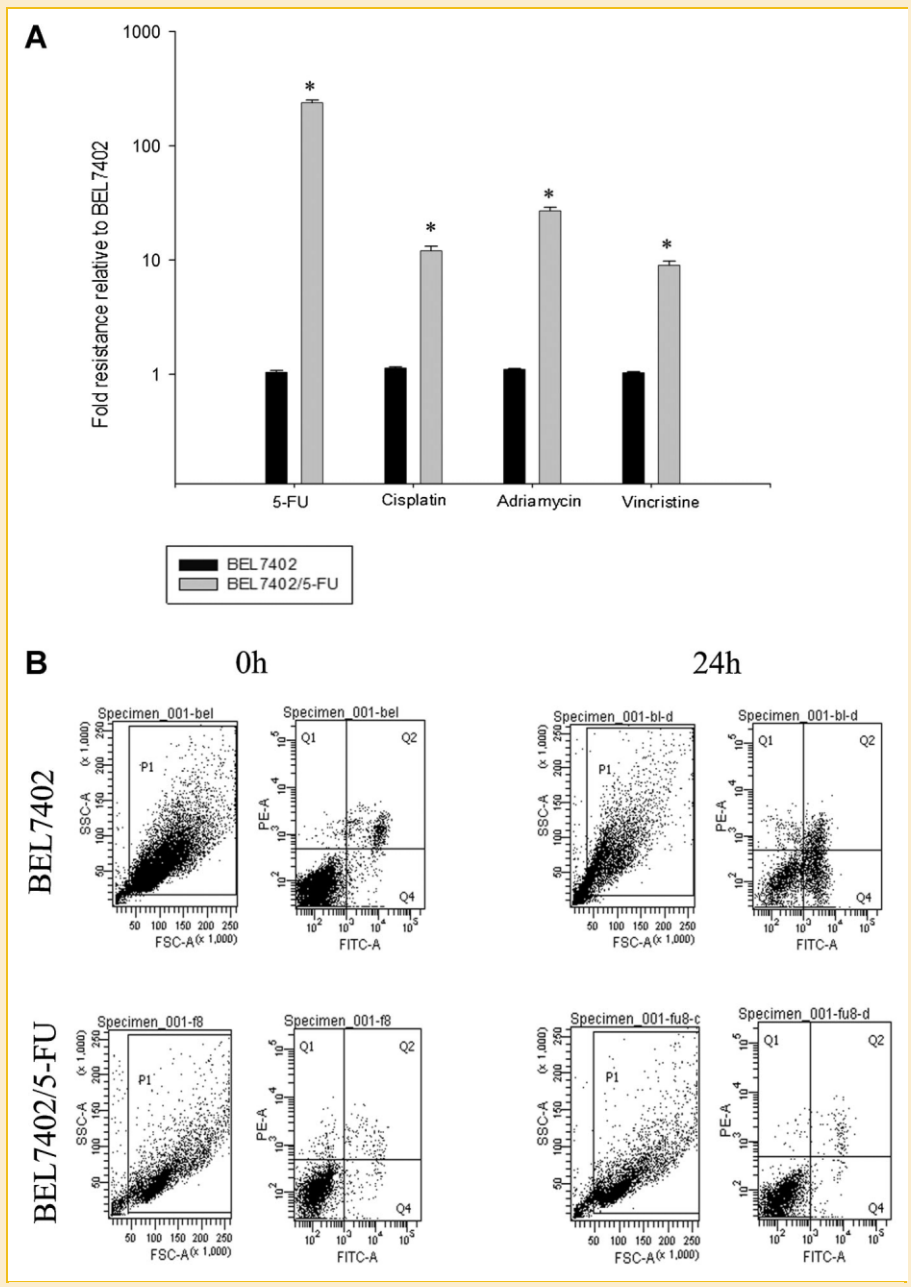


Fig. 1. Biological characteristics of BEL7402/5-FU cells. A: Dose–response curves were plotted and analyzed using the probit model in SPSS 10.0 software. The IC50 values for 5-FU treatment in BEL7402/5-FU and BEL7402 cells were 673.77 ± 55.52 mg/L and 2.84 ± 0.36 mg/L, respectively, which meant the resistance of BEL7402/5-FU to 5-FU was 237.24-fold higher than that of BEL7402 cells. In addition, BEL7402/5-FU also displays cross-resistance to cisplatin, adriamycin, and vincristine. Bars, represent standard deviation (SD). $^{*}P \leq 0.05$ differ from control by *t*-test. B: After treatment with 100 mg/L 5-FU, the apoptotic rate was measured by V-FITC/PI detection on flow cytometry. The apoptotic rate was much higher in BEL7402 cels than in BEL7402/5-FU cells.

model, which would have a potential significance in the study on the MDR mechanism.

### iTRAQ ANALYSIS OF DIFFERENTIALLY EXPRESSED PROTEINS

To investigate the molecular characteristics of MDR in HCC, we employed a quantitative proteomic approach with isobaric labeling (iTRAQ) using the 5-FU resistant human HCC cell line BEL7402/5-FU and its parental cell line BEL7402 as a model. For increasing the coverage of protein identification and/or the confidence of the data generated, samples were iTRAQ labeled in duplicate as follows (100 μg each per label): BEL7402/5-FU, 117; BEL7402/5-FU, 119; BEL7402, 116; BEL7402, 118. The labeled peptide samples were then pooled and dried in a vacuum concentrator. To reduce extreme sample's complexity, a batch of 70 fractions was separated per iTRAQ experiment using strong cation exchange chromatography as described in Materials and Methods Section. These fractions were then combined into 20 samples and analyzed by LC/MS/MS. A schematic flow of the iTRAQ method is shown in Figure 2A. The MS/MS spectrum of ANXA3 (peptide sequence: GAGTNEDALIEILTTR) is illustrated in Figure 2B. 5-FU resistant BEL7402/5-FU cells were labeled with iTRAQ 117 and 119 tags, and BEL7402 cells were labeled with iTRAQ 116 and 118 tags. Thus the ratio of 119:118 and 117:116 would indicate the relative abundance of the ANXA3 protein (Fig. 2B) in BEL7402/5-FU compared with BEL7402 cells, respectively. When the same protein gave two relative quantitative ratios in both 117:116 and 119:118, the quantitation ratio is selected from the experiment with the best *P* values. A total of 660 unique proteins were identified with 95% confidence by the ProteinPilot search algorithm against the IPI human protein database v3.49. Although relative quantification analysis by ProteinPilot 2.0 software come with statistical analysis and since most methods are prone to technical variation, we included an additional 1.3-fold change cutoff for all iTRAQ ratios to reduce false positives for the selection of differentially expressed proteins. This filtering measure resulted in a final set of 52 differentially expressed proteins between BEL7402/5-FU and BEL7402. Of those, 26 proteins

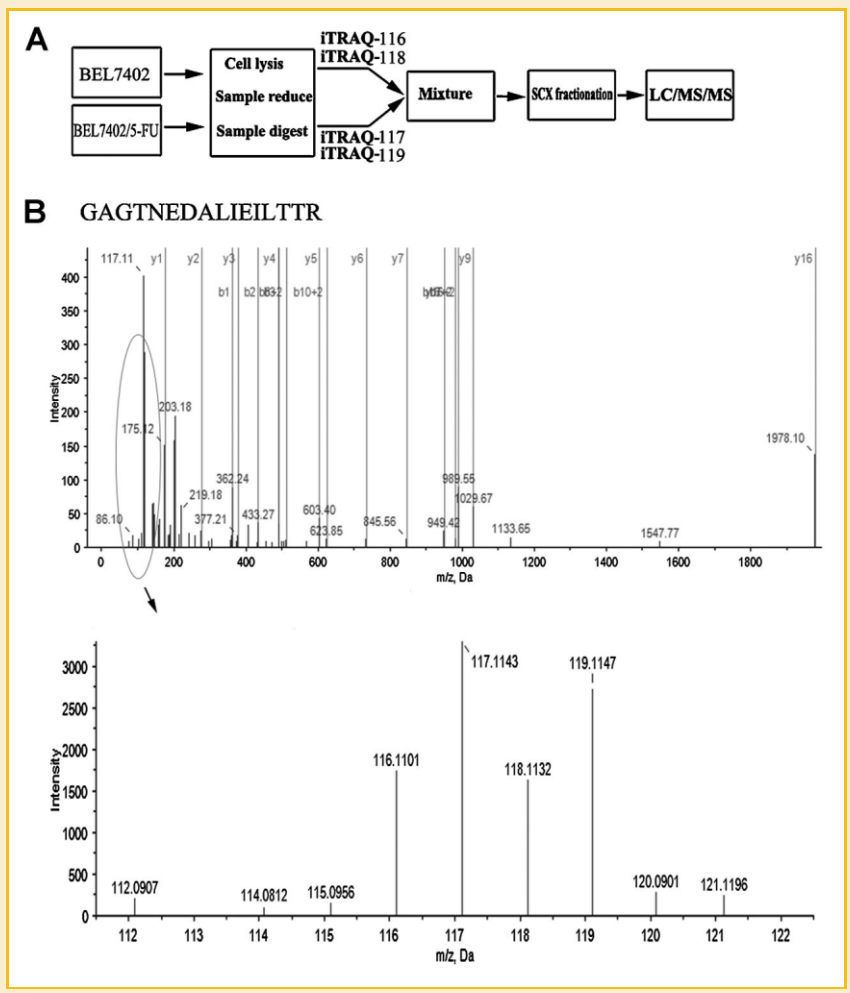


Fig. 2. The iTRAQ proteomics approach was used to identify differentially expressed proteins in BEL7402/5-FU and BEL7402 cells. A: Flow chart of iTRAQ proteomics approach. B: A representative MS/MS spectrum showing the peptides from ANXA3 (peptide sequence: GAGTNEDALIEILTTR). 5-FU resistant BEL7402/5-FU cells were labeled with iTRAQ 117 and 119 tags, and BEL7402 cells were labeled with iTRAQ 116 and 118 tags. Thus the ratio of 119:118 and 117:116 indicated the relative abundance of the ANXA3 protein in BEL7402/5-FU compared with BEL7402 cells.

TABLE II. iTRAQ Analysis of Differentially Expressed Proteins Between 5-FU Resistant BEL7402/5-FU and BEL7402

| Number | Accession | Gene | Protein | BEL7402/5-FU: BEL7402 | PVal (BEL7402/5-FU: BEL7402) | Function |
|---|---|---|---|---|---|---|
| 1 | IPI:IPI00022977.1 | CKB | Creatine kinase B-type | 0.37 | 4.30E−02 | Kinase |
| 2 | IPI:IPI00552873.2 | HIST1H2AI | His tone H2 A type 1-J | 0.65 | 1.88E−11 | Histone |
| 3 | IPI:IPI00419585.9 | PPIA | Peptidyl-prolyl *cis–trans* isomerase A | 0.65 | 1.60E−13 | Chaperone |
| 4 | IPI:IPI00025091.3 | RPS11 | 40S ribosomal protein S11 | 0.68 | 1.39E−02 | Ribosomal protein |
| 5 | IPI:IPI00217465.5 | HIST1H1C | HistoneH1.2 | 0.68 | 1.22E−02 | Histone |
| 6 | IPI:IPI00792410.1 | RPL38 | 8 kDa protein | 0.69 | 5.93E−03 | Ribosomal protein |
| 7 | IPI:IPI00376215.2 | PRKDC | Isoform 2 of DNA-dependent protein kinase catalytic subunit | 0.69 | 1.33E−02 | Nucleotide kinase |
| 8 | IPI:IPI00026215.1 | FEN1 | Flap endonuclease 1 | 0.70 | 2.78E−03 | Acyltransferase |
| 9 | IPI:IPI00030131.3 | TMPO | Isoform beta of lamina-associated polypeptide 2, isoforms beta/gamma | 0.72 | 3.78E−03 | Peptide hormone |
| 10 | IPI:IPI00554538.3 | TPP1 | 60 kDa protein | 0.72 | 2.35E−02 | Serine protease |
| 11 | IPI:IPI00465361.4 | RPL13 | 60S ribosomal protein L13 | 0.72 | 1.32E−04 | Ribosomal protein |
| 12 | IPI:IPI00642402.1 | ATXN2L | 114 kDa protein | 0.72 | 2.66E−02 | RNA banding protein |
| 13 | IPI:IPI00216659.1 | RBM8A | Isoform 2 of RNA-binding protein 8A | 0.73 | 2.66E−02 | RNA banding protein |
| 14 | IPI:IPI00011253.3 | RPS3 | 40S ribosomal protein S3 | 0.73 | 4.14E−06 | Ribosomal protein |
| 15 | IPI:IPI00011200.5 | PHGDH | D-3-phosphoglycerate dehydrogenase | 0.73 | 4.03E−02 | Oxidoreductase activity |
| 16 | IPI:IPI00220362.5 | HSPE1 | 10 kDa heat shock protein, mitochondrial | 0.73 | 7.36E−05 | Chaperone |
| 17 | IPI:IPI00007765.5 | HSPA9 | Stress-70 protein, mitochondrial precursor | 0.74 | 3.61E−06 | Chaperone |
| 18 | IPI:IPI00550239.4 | H1F0 | HistoneH1.0 | 0.75 | 1.89E−02 | Histone |
| 19 | IPI:IPI00398964.2 | LOC728658 | Similar to ribosomal protein L13a | 0.75 | 2.02E−02 | Ribosomal protein |
| 20 | IPI:IPI00433834.2 | RPL26 | Uncharacterized protein RPL26 | 0.75 | 1.83E−02 | Ribosomal protein |
| 21 | IPI:IPI00221091.9 | RPS15A | 40S ribosomal protein S15a | 0.76 | 2.30E−02 | Ribosomal protein |
| 22 | IPI:IPI00219156.7 | RPL30 | 60S ribosomal protein L30 | 0.76 | 9.68E−03 | Ribosomal protein |
| 23 | IPI:IPI00419373.1 | HNRPA3 | Isoform 1 of ribonucleoprotein A3heterogeneous nuclear | 0.77 | 2.51E−03 | DNA-binding protein |
| 24 | IPI:IPI00553164.4 | RPSA | 40S ribosomal protein SA | 0.77 | 4.65E−02 | Ribosomal protein |
| 25 | IPI:IPI00013485.3 | RPS2 | 40S ribosomal protein S2 | 0.77 | 1.89E−02 | Ribosomal protein |
| 26 | IPI:IPI00012069.1 | NQ01 | NAD | 0.77 | 1.55E−02 | Dehydrogenase |
| 27 | IPI:IPI00005162.3 | ARPC3 | Actin-related protein 2/3 complex subunit 3 | 1.30 | 4.00E−02 | Structural protein |
| 28 | IPI:IPI00746310.3 | HMGA1 | Isoform HMG-R of High mobility group protein HMG-I/HMG-Y | 1.30 | 4.11E−04 | DNA-binding protein |
| 29 | IPI:IPI00328170.9 | GCS1 | Mannosyl-oligosaccharide glucosidase | 1.31 | 2.78E−02 | Glucosidase |
| 30 | IPI:IPI00297982.7 | EIF2S3 | Eukaryotic translation initiation factor 2 subunit 3 | 1.32 | 2.07E−02 | Nucleotidyltransferase |
| 31 | IPI:IPI00291510.3 | IMPDH2 | Inosine-5′-monophosphate dehydrogenase 2 | 1.34 | 4.73E−06 | Dehydrogenase |
| 32 | IPI:IPI00796541.1 | ARHGDIA | 26 kDa protein | 1.34 | 4.95E−06 | Signaling molecule |
| 33 | IPI:IPI00302927.6 | CCT4 | T-complex protein 1 subunit delta | 1.34 | 1.26E−02 | Chaperone |
| 34 | IPI:IPI00012007.6 | AHCY | Adenosylhomocysteinase | 1.35 | 4.01E−06 | Hydrolase |
| 35 | IPI:IPI00216298.6 | TXN | Thioredoxin | 1.36 | 4.07E−05 | Oxidoreductase activity |
| 36 | IPI:IPI00008274.7 | CAP1 | Adenylyl cyclase-associated protein 1 | 1.37 | 2.84E−02 | Structural protein |
| 37 | IPI:IPI00015148.3 | RAP1B | Ras-related protein Rap-1b precursor | 1.38 | 2.43E−02 | Signaling molecule |
| 38 | IPI:IPI00514330.5 | HDGF | Hepatoma-derived growth factor | 1.39 | 2.42E−06 | Signaling molecule |
| 39 | IPI:IPI00329801.12 | ANXA5 | Annexin A5 | 1.40 | 1.28E−05 | Calcium-binding proteins |
| 40 | IPI:IPI00295851.4 | COPB1 | Coatomer subunit beta | 1.41 | 6.16E−03 | Vesicle coat protein |
| 41 | IPI:IPI00183695.9 | S100A10 | ProteinS 100-A10 | 1.41 | 3.28E−05 | Calcium-binding proteins |
| 42 | IPI:IPI00746806.1 | CTTN | CTTN protein | 1.42 | 4.83E−04 | Structural protein |
| 43 | IPI:IPI00100160.3 | CAND1 | Isoform 1 of ullin-associated EDD8-dissociated protein 1 | 1.43 | 3.63E−02 | DNA-binding protein |
| 44 | IPI:IPI00027463.1 | S100A6 | Protein S100-A6 | 1.43 | 1.30E−03 | Calcium-binding proteins |
| 45 | IPI:IPI00550900.1 | TPT1 | Translationally controlled tumor protein | 1.45 | 5.47E−04 | Structural protein |
| 46 | IPI:IPI00784161.1 | SUPT6H | Isoform 1 of transcription elongation factor SPT6 | 1.48 | 4.40E−02 | DNA-binding protein |
| 47 | IPI:IPI00642032.1 | TXNL1 | 37 kDa protein | 1.49 | 5.38E−03 | Oxidoreductase activity |
| 48 | IPI:IPI00455315.4 | ANXA2 | Annexin A2 | 1.53 | 1.35E−17 | Calcium-binding proteins |
| 49 | IPI:IPI00010154.3 | GDI1 | Rab GDP dissociation inhibitor alpha | 1.54 | 5.04E−04 | Acyltransferase |
| 50 | IPI:IPI00010214.1 | S100A14 | Protein S100-A14 | 1.67 | 3.80E−02 | Calcium-binding proteins |
| 51 | IPI:IPI00024095.3 | ANXA3 | Annexin A3 | 1.67 | 9.56E−06 | Calcium-binding proteins |
| 52 | IPI:IPI00641181.5 | MARCKSL1 | MARCKS-related protein | 1.93 | 2.02E−02 | Structural protein |

were increased and 26 were decreased in BEL7402/5-FU (Table II). These 52 proteins, which were differentially expressed between the BEL7402/5-FU and BEL7402, could be classified into 13 functional categories using the PANTHER classification system (www.pantherdb.org) (Fig. 3). The top four molecular functions categories were ribosomal protein (19.23%), calcium-binding proteins (11.54%), DNA- or RNA-binding protein (11.54%), and structural protein (9.62%).

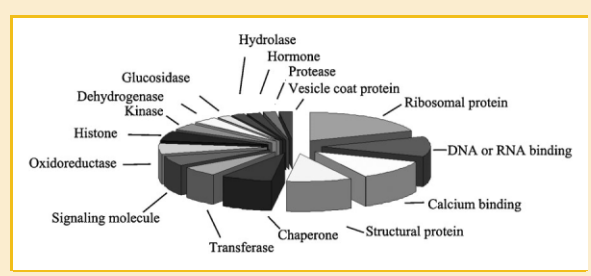


Fig. 3. Pie chart showing the various functional categories as a percentage of the 52 differentially expressed proteins based on the PANTHER classification system.

## VALIDATION OF DIFFERENTIAL EXPRESSION PROTEINS

The differential expression levels of the proteins identified by the iTRAQ approach were validated using Western blot and real-time quantitative RT-PCR analysis. Figure 4A shows the relative mRNA

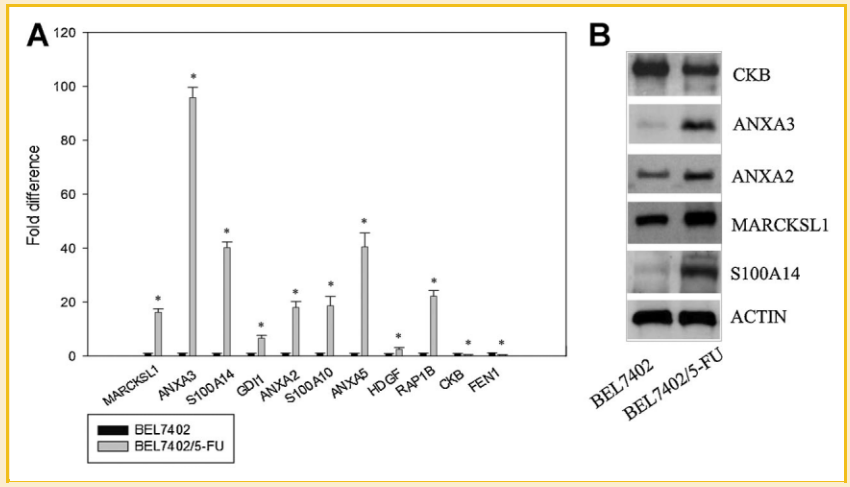


Fig. 4. Evaluation of the differentially expressed proteins in BEL7402/5-FU and BEL7402 cells. A: Real-time RT-PCR detected the relative mRNA expression levels of MARCKSL1, ANXA3, S100A14, GDI1, ANXA2, S100A10, ANXA5, HDGF, RAP1B, CKB, and FEN1. 18S rRNA was used as the normalization standard. Compared with BEL7402, 5-FU resistant BEL7402/5-FU had an obvious up-regulation of MARCKSL1, ANXA3, S100A14, GDI1, ANXA2, S100A10, ANXA5, HDGF, and RAP1B and down-regulation of CKB and FEN1, which were identical with the protein level changes in iTRAQ analysis. Bars, indicate SD. $^{*}P \leq 0.05$ differ from control by *t*-test. B: A representative Western blot analysis result of MARCKSL1, ANXA3, S100A14, ANXA2, and CKB expression in the two cell lines. Compared with BEL7402, BEL7402/5-FU had an obvious up-regulation of MARCKSL1, ANXA3, S100A14, and ANXA2, and a marked down-regulation of CKB.

expression levels of MARCKSL1, ANXA3, S100A14, GDI1, ANXA2, S100A10, ANXA5, HDGF, RAP1B, CKB, and FEN1, as normalized to18S rRNA. The mRNA levels of MARCKSL1, ANXA3, S100A14, GDI1, ANXA2, S100A10, ANXA5, HDGF, and RAP1B, are up-regulated in the 5-FU resistant BEL7402/5-FU, whereas the mRNA level of CKB and FEN1 are down-regulated, as compared to BEL7402. This trend is similar to their protein expression levels obtained in iTRAQ approach. Figure 4B shows representative Western blot analysis results of MARCKSL1, ANXA3, S100A14, ANXA2, and CKB expressions in the two cell lines. Compared with BEL7402, 5-FU resistant BEL7402/5-FU had an obvious up-regulation of MARCKSL1, ANXA3, S100A14, and ANXA2, and a marked down-regulation of CKB.

### THE ASSOCIATION OF ANXA3 WITH MDR

To study the functional role of ANXA3 up-regulation in BEL7402/5-FU, BEL7402/5-FU was transfected with ANXA3 siRNA. Firstly, siRNA-induced inhibition of ANXA3 expression was determined by Western blot analysis. As shown in Figure 5A, transfection of BEL7402/5-FU cells with two ANXA3-specific siRNA sequences, siRNA1 and siRNA2, significantly reduced ANXA3 protein levels, whereas ANXA3 protein expression was not significantly suppressed by transfection of control siRNA. We next evaluated the effect of ANXA3 siRNA transfection on BEL7402/5-FU anti-cancer drug resistance. BEL7402/5-FU cells were treated with ANXA3 siRNA for 2 days, and for additional 72 h incubation with IC50 concentration of selected agents. As shown in Figure 5B, ANXA3 siRNA transfected BEL7402/5-FU cells enhanced the sensitivity to 5-FU, cisplatin, and adriamycin, with the significant decrease of the cell viability, but had no significant effect on vincristine. The above results indicated that the increased expression of ANXA3 in the 5-FU resistant BEL7402/5-FU cells contributed significantly to the observed drug resistance phenotype in these cells.

### RELEVANCE OF ANXA3 TO CLINICAL HEPATOCELLULAR CARCINOMA

The dysregulation of annexins, including ANXA1 and ANXA2, has been reported in multiple neoplasms, suggesting that annexins may play important roles in tumor development and progression, but there have been very few reports on the association of ANXA3 with HCC. Moreover, drug resistance and malignant progression of tumors might be inseparable cellular events. Therefore we investigated whether the up-regulation of ANXA3 could also be observed in clinical samples. To assess the clinical relevance of ANXA3, we examined its expression in 20 matched normal and HCC tissues by IHC. The results showed that ANXA3 was up-regulated in HCC tumor tissues compared with matched normal tissues in 15 out of 20 (75%) patients, and representative images of the IHC are shown in Figure 5C.

## DISCUSSION

Quantitative proteomics has been proved to be a useful technique for investigation of the molecular mechanism in cancer. With regard to iTRAQ analysis, which is currently the most widely used approach for high throughput protein quantitation, enables simultaneous quantification of up to eight different biological samples [Guo et al., 2008]. The aim of this study was to gain insight into the molecular mechanisms of MDR in HCC. So we used iTRAQ proteomic approach to identify proteins with differential expression between the parental drug-sensitive BEL7402 and 5-FU resistant BEL7402/5-FU cells. As a result, 52 proteins were identified with significant

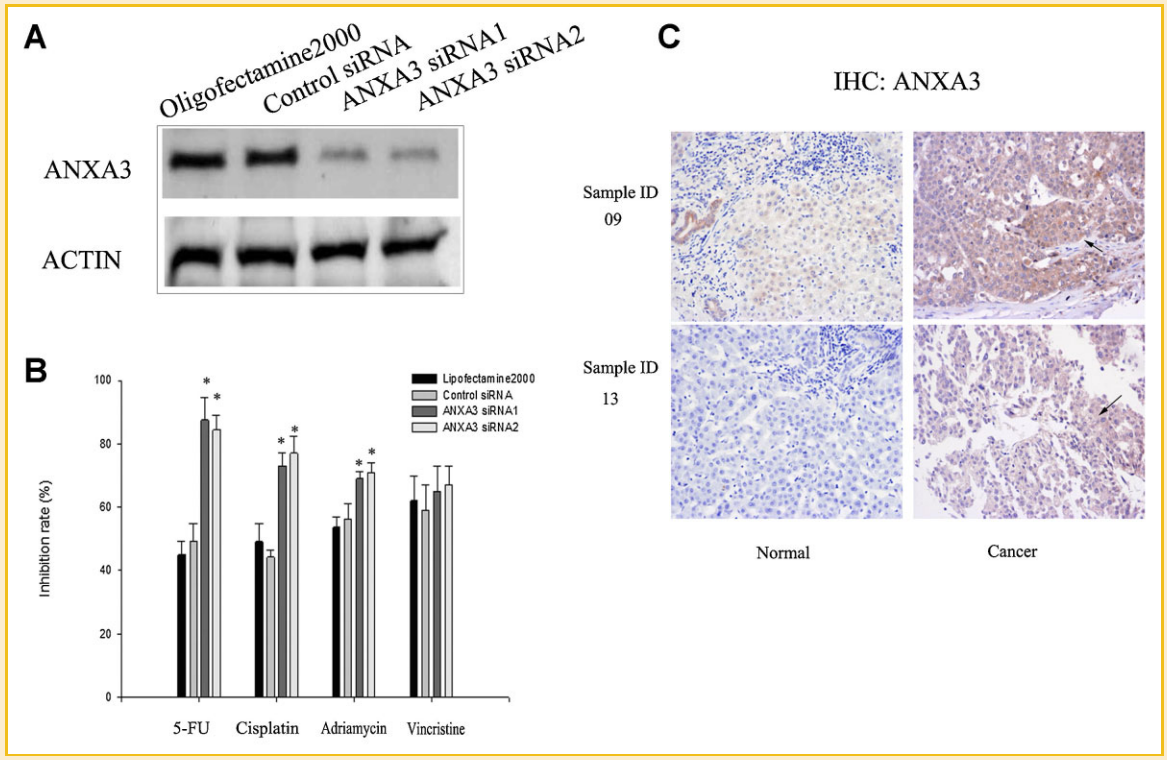


Fig. 5. ANXA3 contributes to the MDR phenotype of BEL-7402/5-FU cells. A: Western blot analysis showed that transfection of BEL7402/5-FU cells with two ANXA3-specific siRNA sequences, siRNA1 and siRNA2, significantly reduced ANXA3 protein levels, whereas ANXA3 protein expressions were not significantly suppressed by control siRNA or transfection reagent alone. B: Suppression of ANXA3 expression enhanced the sensitivity to 5-FU, cisplatin, and adriamycin, with a significantly increased inhibition rate. Bars, indicate SD. $^{*}P \leq 0.05$ differ from control by *t*-test. C: Immunohistochemical assessment of ANXA3 expression in clinical samples showed that ANXA3 was up-regulated in 15 out of 20 (75%) hepatocellular carcinoma patients as compared to matched normal tissues. [Color figure can be seen in the online version of this article, available at http://wileyonlinelibrary.com/journal/jcb]

alterations in expression between the two cell lines. Eleven of these, i.e. MARCKSL1, ANXA3, S100A14, GDI1, ANXA2, S100A10, ANXA5, HDGF, RAP1B, CKB, and FEN1 were confirmed using real-time RT-PCR analysis and Western blot analysis. We further validated the functional role of one protein in drug resistance, ANXA3, which was highly expressed in BEL7402/5-FU cells. Suppression of ANXA3 expression could enhance the sensitivity of BEL7402/5-FU cells to 5-FU. In addition, interestingly enough, our approach led to the further characterization of ANXA3 as highly correlated with the development and progression of clinical HCC, which had never been reported before. It provides evidence that the iTRAQ reagents labeling method for the large scale protein quantification was powerful and reliable. Based on the PANTHER classification system, all the 52 proteins could be classified into 13 functional categories. We discuss some of the key proteins discovered in this work in the following text.

The expressions of six calcium-binding proteins obviously changed in BEL7402/5-FU. ANXA3 is one of the least studied members of the annexin family (I–XIII), which bind to the phospholipids in a $Ca^{2+}$ dependent manner and play a role in the regulation of cellular growth and in signal transduction pathways [Moss and Morgan, 2004]. It can mediate angiogenesis, possibly through enhancing hypoxia-inducible factor-1 (HIF-1) transactivation activity and stimulating vascular endothelial growth factor (VEGF) production, suggesting that ANXA3 might play critical roles in the progress of diseases such as tumor growth [Park et al., 2005]. ANXA3 has also been shown to play an important role in rat liver regeneration through a hepatocyte growth factor-mediated pathway [Harashima et al., 2008]. Furthermore it is described that cytotoxic drug OSU03013, a derivative of celecoxib, exhibits its antitumor activity by decreasing ANXA3 expression in lung cancer cell lines, and over-expression of ANXA3 is detected in platinum-resistant human ovarian cancer cells [Tan et al., 2008; Yan et al., 2007]. To date, a rational correlation of ANXA3 with MDR remains unknown. However, in this study ANXA3 was observed to be over-expressed in 5-FU resistant BEL7402/5-FU cells. The mRNA level of ANXA3 gene was also higher almost 100 folds in BEL7402/5-FU than in BEL7402. In addition, we demonstrated that the suppression of ANXA3 expression in BEL7402/5-FU can enhance the sensitivity to 5-FU, cisplatin, and adriamycin. Taken together, these data reveal for the first time that ANXA3 was involved in the MDR phenotype of BEL7402/5-FU. Coupled to the existing knowledge on the functional roles of ANXA3 in cancer, we hypothesized that ANXA3 may contribute to MDR through enhancing HIF-1 transactivation activity, which could prompt MDR phenotype via inhibition of drug-induced apoptosis and decreases in intracellular drug accumulation [Liu et al., 2008]. Among annexins, reports on the association of ANXA3 with HCC are very few. Moreover, drug resistance and malignant progression of tumors might be inseparable cellular events [McMillan and Hart, 1987]. Therefore,

we further evaluated the expression of ANXA3 in 20 matched normal and HCC tissues by IHC. Our results demonstrated that almost 75% of the clinical HCC samples showed over-expression of ANXA3, suggesting that ANXA3 is a promising candidate for future biomarker development and as a novel drug target for HCC. However, no statistically significant differences were observed in the expression of ANXA3 between the cancer subtypes and different stages—suggesting that ANXA3 may not be related to oncogenesis but required for cancer maintenance or progression.

Among the identified structural proteins, the levels of translationally controlled tumor protein (TPT1) were markedly increased in BEL7402/5-FU. TPT1 is an anti-apoptotic protein that is highly expressed in several cancer cells including liver cancer [Li et al., 2001]. Expression of TPT1 is up-regulated by various stimulus including dioxin, heavy metals, and growth factors [Sturzenbaum et al., 1998; Vercoutter-Edouart et al., 2001; Oikawa et al., 2002]. In addition, TPT1 can act as a tubulin-binding protein, affecting microtubule dynamics during G1-, S-, G2-, and early M-phases of the cell cycle, and mediating microtubule stabilization [Yarm, 2002]. It is well known that cytoskeletal disruption is an early and central process in injury of chemotherapeutic agents such as cisplatin, vincristine, and adriamycin. It is possible that TPT1 may interact with the cytoskeleton after drug injury, thereby protecting cancer cells from specific manifestations of sublethal injury.

Our study also found that hepatoma-derived growth factor (HDGF), a member of the heparin-binding growth factor family, was over-expressed in 5-FU resistant cell line BEL7402/5-FU. A recent study indicated that HDGF might act as a survival factor and its knock-down was found to not only induce the expression of the pro-apoptotic protein Bad but also inactivate ERK and Akt, which in turn led to dephosphorylation of Bad at Ser-112 and Ser-136, and activation of the intrinsic apoptotic pathway [Tsang et al., 2008]. Subsequent studies showed over-expression of HDGF enhances the cell resistance to NDGA, a novel chemotherapeutic agent for cancer, via the inhibition of mitochondria apoptotic pathway, which is an important mechanism of drug resistance [Liao et al., 2010]. Thus, HDGF is considered to be strongly correlated with chemotherapeutic resistance.

IMPDH gene encodes the rate-limiting enzyme in the de novo guanine nucleotide biosynthesis, maintaining the cellular guanine deoxynucleotide and ribonucleotide pools needed for DNA and RNA synthesis [Zimmermann et al., 1996]. IMPDH type I is constitutively expressed in normal cells, whereas IMPDH type II activity has been shown to be increased in proliferating and especially malignant cells [Zimmermann et al., 1996, 1998]. IMPDH2 has been shown to be over-expressed in methotrexate (MTX) treated and resistant cells. Furthermore, inhibition of IMPDH activity sensitized these cells to MTX cytotoxicity, suggesting that IMPDH could constitute a target to develop modulators in MTX chemotherapy [Penuelas et al., 2005]. Subsequent investigations showed that IMPDH2 over-expression induces a strong chemoresistance in osteosarcoma cells which is mediated at least in part by increased expression of anti-apoptotic proteins [Fellenberg et al., 2010]. The up-regulated IMPDH2 protein in drug resistant cell line BEL7402/5-FU was also discovered in this study, suggesting that IMPDH2 might be directly involved in the development of chemoresistance in HCC.

Finally, our study identified several proteins, including ANXA2, MARCKSL1, S100A14, and S100A6, which had not been associated with MDR previously, but had been implicated in tumor progression through enhancing angiogenesis, tumor invasion and metastasis [Finlayson and Freeman, 2009; Nedjadi et al., 2009; Zhang et al., 2009; Wang et al., 2010]. Recent studies showed that acquisition of MDR phenotype is often associated with an elevated invasion/metastasis of tumor [Kerbel et al., 1994]. Our results supported that development of MDR not only prohibits effective chemotherapy, but also exacerbates the metastatic symptom of cancer patients. The correlation between each of the differentially expressed proteins and MDR in BEL7402/5-FU will be subjected to future study.

Resistance to anti-cancer drugs is one of major problems faced during chemotherapy of HCC, but the mechanism underlying MDR is still unclear. In this study, we focused our attention on those proteins that changed in expression levels in 5-FU resistant cell line BEL7402/5-FU. As a result, 52 differentially expressed proteins possibly associated with MDR of BEL7402/5-FU were identified, and the correlation of ANXA3 with MDR was verified. These data were valuable for further to study the mechanism of MDR in human HCC, and also provide some new clues for investigating other tumors MDR.

## ACKNOWLEDGMENTS

This work was supported by program for Changjiang Scholars and Innovative Research Team in University (no. IRT0872), National Natural Science Foundation of China (no. 30930082, 30771923, 30801348, and 30900507), National Science and Technology Major Project of China (no. 2008ZX10002-006), and China Postdoctoral Science Foundation Founded Project (no. 20070410210).

## REFERENCES

Fellenberg J, Kunz P, Sahr H, Depeweg D. 2010. Overexpression of inosine 5′-monophosphate dehydrogenase type II mediates chemoresistance to human osteosarcoma cells. PloS One 5:e12179.

Finlayson AE, Freeman KW. 2009. A cell motility screen reveals role for MARCKS-related protein in adherens junction formation and tumorigenesis. PloS One 4:e7833.

Flick DA, Gifford GE. 1984. Comparison of in vitro cell cytotoxic assays for tumor necrosis factor. J Immunol Methods 68:167–175.

Fu C, Wu C, Liu T, Ago T, Zhai P, Sadoshima J, Li H. 2009. Elucidation of thioredoxin target protein networks in mouse. Mol Cell Proteomics 8:1674–1687.

Guo T, Gan CS, Zhang H, Zhu Y, Kon OL, Sze SK. 2008. Hybridization of pulsed-Q dissociation and collision-activated dissociation in linear ion trap mass spectrometer for iTRAQ quantitation. J Proteome Res 7:4831–4840.

Harashima M, Harada K, Ito Y, Hyuga M, Seki T, Ariga T, Yamaguchi T, Niimi S. 2008. Annexin A3 expression increases in hepatocytes and is regulated by hepatocyte growth factor in rat liver regeneration. J Biochem 143:537–545.

Ho J, Kong JW, Choong LY, Loh MC, Toy W, Chong PK, Wong CH, Wong CY, Shah N, Lim YP. 2009. Novel breast cancer metastasis-associated proteins. J Proteome Res 8:583–594.

Jin J, Huang M, Wei HL, Liu GT. 2002. Mechanism of 5-fluorouracil required resistance in human hepatocellular carcinoma cell line Bel (7402). World J Gastroenterol 8:1029–1034.

Kerbel RS, Kobayashi H, Graham CH. 1994. Intrinsic or acquired drug resistance and metastasis: Are they linked phenotypes? J Cell Biochem 56:37–47.

Kusuhara H, Suzuki H, Terasaki T, Kakee A, Lemaire M, Sugiyama Y. 1997. P-Glycoprotein mediates the efflux of quinidine across the blood-brain barrier. J Pharmacol Exp Ther 283:574–580.

Li F, Zhang D, Fujise K. 2001. Characterization of fortilin, a novel anti-apoptotic protein. J Biol Chem 276:47542–47549.

Liao F, Liu M, Lv L, Dong W. 2010. Hepatoma-derived growth factor promotes the resistance to anti-tumor effects of nordihydroguaiaretic acid in colorectal cancer cells. Eur J Pharmacol 645:55–62.

Liu L, Ning X, Sun L, Zhang H, Shi Y, Guo C, Han S, Liu J, Sun S, Han Z, Wu K, Fan D. 2008. Hypoxia-inducible factor-1 alpha contributes to hypoxia-induced chemoresistance in gastric cancer. Cancer Sci 99:121–128.

Livak KJ, Schmittgen TD. 2001. Analysis of relative gene expression data using real-time quantitative PCR and the 2(-Delta Delta C (T)) Method. Methods 25:402–408.

McMillan TJ, Hart IR. 1987. Can cancer chemotherapy enhance the malignant behaviour of tumours? Cancer Metast Rev 6:503–519.

Morrow CS, Diah S, Smitherman PK, Schneider E, Townsend AJ. 1998. Multidrug resistance protein and glutathione S-transferase P1-1 act in synergy to confer protection from 4-nitroquinoline 1-oxide toxicity. Carcinogenesis 19:109–115.

Morrow CS, Smitherman PK, Townsend AJ. 2000. Role of multidrug-resistance protein 2 in glutathione S-transferase P1-1-mediated resistance to 4-nitroquinoline 1-oxide toxicities in HepG2 cells. Mol Carcinog 29:170–178.

Moss SE, Morgan RO. 2004. The annexins. Genome Biol 5:219.

Nedjadi T, Kitteringham N, Campbell F, Jenkins RE, Park BK, Navarro P, Ashcroft F, Tepikin A, Neoptolemos JP, Costello E. 2009. S100A6 binds to annexin 2 in pancreatic cancer cells and promotes pancreatic cancer cell motility. Br J Cancer 101:1145–1154.

Oikawa K, Ohbayashi T, Mimura J, Fujii-Kuriyama Y, Teshima S, Rokutan K, Mukai K, Kuroda M. 2002. Dioxin stimulates synthesis and secretion of IgE-dependent histamine-releasing factor. Biochem Biophys Res Commun 290:984–987.

Park JE, Lee DH, Lee JA, Park SG, Kim NS, Park BC, Cho S. 2005. Annexin A3 is a potential angiogenic mediator. Biochem Biophys Res Commun 337: 1283–1287.

Parkin DM, Bray F, Ferlay J, Pisani P. 2001. Estimating the world cancer burden: Globocan 2000. International journal of cancer. J Int Cancer 94:153–156.

Penuelas S, Noe V, Ciudad CJ. 2005. Modulation of IMPDH2, survivin, topoisomerase I and vimentin increases sensitivity to methotrexate in HT29 human colon cancer cells. FEBS J 272:696–710.

Perez-Tomas R. 2006. Multidrug resistance: Retrospect and prospects in anti-cancer drug treatment. Curr Med Chem 13:1859–1876.

Plumb JA, Milroy R, Kaye SB. 1989. Effects of the pH dependence of 3-(4,5-dimethylthiazol-2-yl)-2,5-diphenyl-tetrazolium bromide-formazan absorption on chemosensitivity determined by a novel tetrazolium-based assay. Cancer Res 49:4435–4440.

Rangiah K, Tippornwong M, Sangar V, Austin D, Tetreault MP, Rustgi AK, Blair IA, Yu KH. 2009. Differential secreted proteome approach in murine model for candidate biomarker discovery in colon cancer. J Proteome Res 8:5153–5164.

Schwartz JD, Schwartz M, Mandeli J, Sung M. 2002. Neoadjuvant and adjuvant therapy for resectable hepatocellular carcinoma: Review of the randomised clinical trials. Lancet Oncol 3:593–603.

Sturzenbaum SR, Kille P, Morgan AJ. 1998. Identification of heavy metal induced changes in the expression patterns of the translationally controlled tumour protein (TCTP) in the earthworm *Lumbricus rubellus*1. Biochim Biophys Acta 1398:294–304.

Tan YH, Lee KH, Lin T, Sun YC, Hsieh-Li HM, Juan HF, Wang YC. 2008. Cytotoxicity and proteomics analyses of OSU03013 in lung cancer. Clin Cancer Res 14:1823–1830.

Tsang TY, Tang WY, Tsang WP, Co NN, Kong SK, Kwok TT. 2008. Down-regulation of hepatoma-derived growth factor activates the Bad-mediated apoptotic pathway in human cancer cells. Apoptosis 13:1135–1147.

Vercoutter-Edouart AS, Czeszak X, Crepin M, Lemoine J, Boilly B, Le Bourhis X, Peyrat JP, Hondermarck H. 2001. Proteomic detection of changes in protein synthesis induced by fibroblast growth factor-2 in MCF-7 human breast cancer cells. Exp Cell Res 262:59–68.

Wang HY, Zhang JY, Cui JT, Tan XH, Li WM, Gu J, Lu YY. 2010. Expression status of S100A14 and S100A4 correlates with metastatic potential and clinical outcome in colorectal cancer after surgery. Oncol Rep 23:45–52.

Yan XD, Pan LY, Yuan Y, Lang JH, Mao N. 2007. Identification of platinum-resistance associated proteins through proteomic analysis of human ovarian cancer cells and their platinum-resistant sublines. J Proteome Res 6:772–780.

Yang YX, Chen ZC, Zhang GY, Yi H, Xiao ZQ. 2008. A subcelluar proteomic investigation into vincristine-resistant gastric cancer cell line. J Cell Biochem 104:1010–1021.

Yang Y, Lim SK, Choong LY, Lee H, Chen Y, Chong PK, Ashktorab H, Wang TT, Salto-Tellez M, Yeoh KG, Lim YP. 2010. Cathepsin S mediates gastric cancer cell migration and invasion via a putative network of metastasis-associated proteins. J Proteome Res 9:4767–4778.

Yarm FR. 2002. Plk phosphorylation regulates the microtubule-stabilizing protein TCTP. Mol Cell Biol 22:6209–6221.

Zhang F, Zhang L, Zhang B, Wei X, Yang Y, Qi RZ, Ying G, Zhang N, Niu R. 2009. Anxa2 plays a critical role in enhanced invasiveness of the multidrug resistant human breast cancer cells. J Proteome Res 8:5041–5047.

Zimmermann A, Gu JJ, Spychala J, Mitchell BS. 1996. Inosine monophosphate dehydrogenase expression: Transcriptional regulation of the type I and type II genes. Adv Enzyme Regul 36:75–84.

Zimmermann AG, Gu JJ, Laliberte J, Mitchell BS. 1998. Inosine-5′-monophosphate dehydrogenase: Regulation of expression and role in cellular proliferation and T lymphocyte activation. Prog Nucleic Acid Res Mol Biol 61:181–209.